Optimal feeding strategy of diafiltration buffer in batch membrane processes

R. Paulen, M. Fikar, G. Foley, Z. Kovacs, P. Czermak

Published Version Information

Citation: Paulen, R., Fikar, M., Foley, G., Kovacs, Z., & Czermak, P. (2012). Optimal feeding strategy of diafiltration buffer in batch membrane processes. Journal of Membrane Science, 411-412, 160-172.

Digital Object Identifier (DOI): doi:10.1016/j.memsci.2012.04.028

Publisher's Link: http://www.sciencedirect.com/science/article/pii/S0376738812003286

Optimal feeding strategy of diafiltration buffer in batch membrane processes

R. Paulen[a,*], M. Fikar[a], G. Foley[b], Z. Kovács[c], P. Czermak[c,d]

[a]*Faculty of Chemical and Food Technology, Slovak University of Technology in Bratislava, Radlinskeho 9, Bratislava, Slovakia*
[b]*School of Biotechnology, Dublin City University, Dublin, Ireland*
[c]*Institute of Bioprocess Engineering and Pharmaceutical Technology, University of Applied Sciences Mittelhessen, Wiesenstrasse 14, 35390 Giessen, Germany*
[d]*Department of Chemical Engineering, Kansas State University, Manhattan, Kansas, USA*

Abstract

This work addresses the optimal control strategy of diafiltration buffer utilisation in discontinuous membrane processes that are designed to fulfil the twin aims of concentration and fractionation. The problem of optimal process operation is formulated using a general membrane response model that encounters concentration-dependent flux and rejections. We consider two problems, operation time minimisation and diluant consumption minimisation, and we apply theory of optimal control and derive necessary conditions of optimality. Through selected case studies from literature, we demonstrate how to apply the proposed methodology to determine optimal time-dependent wash-water feeding policy. The analytical results are confirmed by numerical computations, using numerical methods of dynamic optimisation. The presented methodology allows decision makers to analyse suboptimality of conventional diafiltration strategies in terms of processing time and diluant consumption. Results show that depending on the complexity of the membrane response model, it may be attractive to implement optimal trajectory.

Keywords: modelling, diafiltration, discontinuous operation, optimal control, dynamic optimisation

1. Introduction

Membrane filtration offers a unique separation solution since it can be used for both concentration and fractionation purposes. This feature is described by Jönsson et al. in their review paper on ultrafiltration applications as "Killing two birds with one stone" [1]. In many applications, this characteristics puts membrane filtration in an attractive position and compares favourably with other separation techniques or even with a sequence of competitive unit operations.

*Corresponding author. Tel.: +421 259 325 730; fax: +421 259 325 340.
Email address: radoslav.paulen@stuba.sk (R. Paulen)

A membrane filtration plant can be designed for continuous or batch operation. This work deals with the latter. In comparison with continuous processes, batch operations allow to use membranes with reduced area in order to reach the target product quality, that usually leads to smaller space requirement and lower investment costs [2]. Moreover, batch processing is particularly suited to applications where the process liqueur is manufactured in batches or lots before any subsequent separation is undertaken.

A schematic diagram of a discontinuous membrane diafiltration process is shown in Figure 1. Considering a process liqueur with two solutes, the general purpose of such

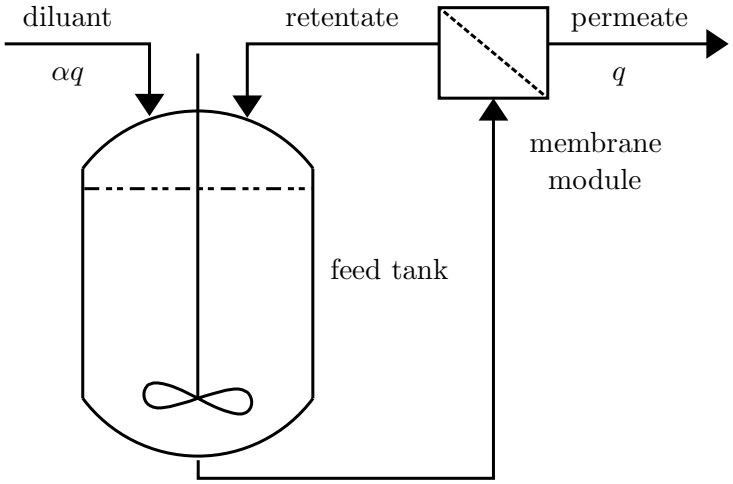

Figure 1: Schematic representation of a generalized batch diafiltration process.

batch plant can be summarized as to increase the macro-solute concentration from $c_{1,0}$ to $c_{1,\mathrm{f}}$ and to reduce the micro-solute concentration from $c_{2,0}$ to $c_{2,\mathrm{f}}$. The fractionation is accomplished by performing a so called *diafiltration* mode in which the micro-solute is washed out of the process liqueur by introducing fresh buffer (i.e. diluant) into the feed reservoir while simultaneously removing the macro-solute-free permeate.

Most filtration processes operate with constant transmembrane pressure that is achieved by simply adjusting the pressure with the retentate valve. We note here that other types of process control strategies, such as constant flux or constant wall concentration control, are also implemented in engineering practice. These are normally preferred when unfavourable effects such as enhanced fouling or product quality deterioration are associated with high concentration of retained species at the membrane wall. For instance, when animal cell damage [3] or denaturation/adsorption of high-value protein pharmaceuticals [4] are of major concern. The work presented here examines the constant pressure approach.

Batch processing can be performed in different ways depending on how the addition of the diluant (diafiltration or washing solvent) into the feed tank is scheduled. The standard way of reaching the dual objective of fractionation and concentration is to perform a multi-step process including pre-concentration (C), constant-volume diafiltration (CVD), and post-concentration steps. Other strategies include variable-volume diafiltration (VVD) [5],

or a variation of it, pre-concentration followed by variable-volume diafiltration (C-VVD) [6]. These processes are best described with α (i.e. the ratio of diluant flow to permeate flow) as a function of operation time as shown in Figure 2.

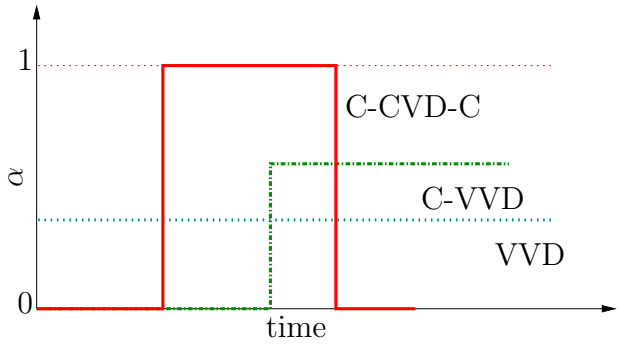

Figure 2: Representation of classical three-step processing (C-CVD-C), pre-concentration combined with variable-volume diafiltration (C-VVD), and variable-volume diafiltration (VVD) operation in terms of the α function.

As it has been pointed out in [7], the best time-varying profile of the diluant addition needs not necessarily be one of the pre-defined profiles depicted in Figure 2. The optimal control trajectory of $\alpha(t)$ (or equivalently the diluant flow) can be determined by formulating an optimization problem subject to process model described by a set of differential equations. The diafiltration process, that is designed by the evaluation of the optimal time-varying profile of the diluant flow, has been then referred to as dynamic-volume diafiltration (DVD).

The wash-water utilisation strategy of DVD may differ from conventional diafiltration processes. However, in many cases it may be attractive to implement the optimal trajectory since it can lead to reduced operation time, diluant consumption, and product losses. The issue of product losses becomes only important when we have to deal with incomplete macro-solute rejections, while the diluant consumption and operation time are generally of major concern. Batch production takes place periodically; when the production is complete, the plant and equipment are available for the next batch. Processing time is a key factor to increase production throughput. Moreover, diafiltration is commonly associated with high consumption of diafiltration solvent. This liquid is commonly water with strict quality requirements regarding bacteriological contamination and organic/inorganic solute content [8]. Thus, the production of diafiltration liquid can contribute significantly to the overall operating costs of the plant.

As far as time minimisation problem considered, it has been previously demonstrated that optimum diafiltration strategy can be found for filtration processes operating in discontinuous manner. The patent [9] issued by the Millipore Co. provides an implementation procedure and a general formula for determining the optimal diafiltration path using idea of maximization of mass flux of permeable component through the membrane. Despite that this approach provides certain level of intuition and insight on time-optimal filtration control, its extendability onto different optimisation tasks and more complex process

setups is questionable.

This work can be thought as a generalisation of our previous contributions [10] where time optimal operation for special case with limiting flux model was investigated and of [11] where numerical procedures for albumin production optimisation were applied. Here we address problems of both minimisation of operational time and diluant consumption for a large class of processes. We will show in specific cases that numerical optimisation can be avoided and give concrete recipes to operate the process optimally. In a general case, we will propose a numerical optimisation procedure of much simpler structure than in [7].

In Sect. 2, we present a general process model and formulate the optimal control problem. Then, we apply the theory of optimal control exploiting the Pontryagin's minimum principle to find optimal control strategy of diluant utilization. We discuss the general case and several specific cases of rejection coefficients (constant, concentration-dependent, complete, or incomplete rejection of macro- and micro-solutes) that are common in membrane filtration practice. Finally, through selected case studies from literature, including reverse osmosis (RO), ultrafiltration (UF), and nanofiltration (NF) applications, we demonstrate how to apply the presented methodology to determine optimal control of batch filtration processes.

2. Model development

We consider a membrane filtration plant (RO, UF, NF, or MF) with a given membrane area that operates under fixed operating conditions. The studied filtration system applies a cross-flow and pressure setpoint, and the permeate flows uncontrolled out of the module. We assume a solution with two species with concentrations c_1, c_2. We assume that the system is well-mixed, and the introduction of diluant causes no local concentration differences. The balance of each solute can be written as

$$\frac{\mathrm{d}c_i}{\mathrm{d}t} = \frac{c_i q}{V}(R_i - \alpha), \quad c_i(0) = c_{i0}, \quad i = 1, 2 \tag{1}$$

where V is the retentate volume at time t. The rejection coefficient $R_i(c_1, c_2)$ is assumed to be a function of both concentrations. The same holds for the permeate flowrate $q(c_1, c_2)$. The volume balance can be written as

$$\frac{\mathrm{d}V}{\mathrm{d}t} = (\alpha - 1)q, \quad V(0) = V_0. \tag{2}$$

Note that the time-dependent variables (i.e. permeate flux and the solute rejections) are solely a function of feed concentrations in the process model. Thus, the model in its current form does not encounter changes in process parameters (pressure, temperature, hydrodynamic conditions, etc.) that might influence the membrane response during the process run. Furthermore, the model is limited to applications where fouling is not pronounced. This means that the findings are restricted to applications where (i) fouling does not occur, (ii) the impact of fouling on flux is sufficiently less than the impact induced by changes in feed composition, or (iii) fouling occurs rapidly within the time-scale of the entire process, and Eqs. (1) and (2) representing the fouled membrane are given.

2.1. Problem formulation

In this section, two different process optimisation problems are introduced. The first one represents a traditional minimum time problem. In this problem, optimal trajectory of function $\alpha(t)$ is computed in order to minimise running time of a batch diafiltration process. The second considers minimisation of diluant consumption during the diafiltration process.

2.1.1. Minimum time problem

The objective of this optimisation task is to find the time-dependent function $\alpha(t)$ which uses minimum time to drive the process from initial state to a prescribed terminal state. Mathematical formulation of this dynamic optimisation problem is as follows

$$J_1 = \min_{\alpha(t)} t_\mathrm{f} = \min_{\alpha(t)} \int_0^{t_\mathrm{f}} 1 \,\mathrm{d}t. \tag{3a}$$

s.t.

$$\dot{c}_1 = \frac{c_1 q}{V}(R_1 - \alpha), \qquad c_1(0) = c_{1,0}, \qquad c_1(t_\mathrm{f}) = c_{1,\mathrm{f}}, \tag{3b}$$

$$\dot{c}_2 = \frac{c_2 q}{V}(R_2 - \alpha), \qquad c_2(0) = c_{2,0}, \qquad c_2(t_\mathrm{f}) = c_{2,\mathrm{f}}, \tag{3c}$$

$$\dot{V} = (\alpha - 1)q, \qquad V(0) = V_0, \tag{3d}$$

$$\alpha \in [\alpha_\mathrm{min}, \alpha_\mathrm{max}] \tag{3e}$$

where α_min and α_max represent lower and upper constraints on the value of α respectively. Lower bound, α_min, obviously stands for pre/post-concentration mode when $\alpha = 0$. Value of upper constraint, α_max, may vary from one application to another. Some applications require that α does not overcome 1.

Other ones do not impose any upper bound on the value of α which in principle means that $\alpha_\mathrm{max} = \infty$. This can have a special meaning if it happens at the beginning or at the end of the operation. We will speak about a pure dilution mode where a certain volume of diluant is added into the system instantaneously. This can happen in a separate equipment not related to membrane equipment.

2.1.2. Minimum diluant problem

The second problem addresses minimisation of total amount of diluant $u(t) = \alpha(t)q(t)$ used to drive the process from initial state to a prescribed terminal state assuming that the final time t_f is a free variable. Mathematical formulation (3) remains unchanged in this case except for the cost function

$$J_2 = \min_{\alpha(t)} \int_0^{t_\mathrm{f}} \alpha(t)q(t) \,\mathrm{d}t. \tag{4}$$

3. Main results

A detailed mathematical derivation of the main results is described in Appendix A. Here we present them in compact way. We will at first treat the complete rejection of

the macro-solute ($R_1 = 1$). This will give us complete analytical characterization of the optimal control operation. Next, we will treat the general case. Here, we will show that the optimal operation can de determined from an optimization problem of much simpler structure than derived previously in [7, 11].

3.1. Complete rejection of macro-solute

This is a special case from the theoretical point of view. However, this condition is in practice satisfied almost always and it is thus not very restrictive.

Both studied problems (minimum time and minimum diluant) require that concentrations lie on the optimal surface $S(c_1, c_2)$ given as

$$S_{\text{time}}(c_1, c_2) = (R_2 - 1)\left(q + c_1\frac{\partial q}{\partial c_1} + c_2\frac{\partial q}{\partial c_2}\right) + q\left(c_1\frac{\partial R_2}{\partial c_1} + c_2\frac{\partial R_2}{\partial c_2}\right) = 0, \tag{5}$$

$$S_{\text{diluant}}(c_1, c_2) = R_2 - 1 + c_1\frac{\partial R_2}{\partial c_1} + c_2\frac{\partial R_2}{\partial c_2} = 0. \tag{6}$$

We note that Eq. (5) is consistent with maximization of mass flux through the membrane considered in [9].

The optimal control strategy α that will keep the concentrations on this surface can be calculated as

$$\alpha(c_1, c_2) = \frac{\frac{\partial S}{\partial c_1}c_1R_1 + \frac{\partial S}{\partial c_2}c_2R_2}{\frac{\partial S}{\partial c_1}c_1 + \frac{\partial S}{\partial c_2}c_2}. \tag{7}$$

The overall optimal operation can be stated as follows:

1. The first step is either pure concentration ($\alpha = 0$) or operation with $\alpha = \alpha_{\max}$ until the condition $S(c_1, c_2) = 0$ is met.
2. The second step is filtration with time-dependent $\alpha(c_1, c_2)$ given by (7) maintaining optimal concentration values.
3. Finally, the third step is again either pure concentration ($\alpha = 0$) or operation with $\alpha = \alpha_{\max}$ until final concentrations of both components are obtained.

Any of these three steps can be missing at a particular problem, depending on process initial and final conditions as well as actual functions $R_2(c_1, c_2)$, $q(c_1, c_2)$. For the most common case $R_1 = 1$, $R_2 = 0$ and the minimum diluant problem, it follows from (6) that the optimal surface will never be reached and the optimal control will be attained by α on its constraints, so called bang-bang control.

The optimal surface in the minimum time problem (5) reduces for the most common case $R_1 = 1$, $R_2 = 0$ to

$$S_{\text{time}}(c_1, c_2) = q + c_1\frac{\partial q}{\partial c_1} + c_2\frac{\partial q}{\partial c_2} = 0. \tag{8}$$

3.2. General case

In the general case we do not know the optimal concentration surface and have to apply numerical techniques of dynamic optimization to solve our problem. However, we can use results derived in Appendix A to simplify it.

We form a problem of non-linear programming with five unknowns $\Delta t_1, \Delta t_2$, and Δt_3 being the lengths of time intervals of the respective phases and α_1 and α_3 being the constant values of α in the first and third phases. Optimal value of α_1 and α_3 will either be on minimum or on maximum. In the second phase, optimal α will be given by (A.22) for the minimum time problem and by (A.29) for the minimum diluant problem. See our previous papers [7, 11] for the survey of numerical methods that can solve this non-linear programming problem. Once it is solved numerically, we know all needed information about optimal operation to apply it to the process.

4. Discussion and case studies

In this section we determine the optimal control strategies where the permeate flux is given by some well-known models, including the limiting flux and osmotic pressure. We then examine five case studies from the literature where the flux is predicted by empirical models specific to the system in question.

4.1. Optimisation at the limiting flux

Let us consider a membrane plant that operates under limiting flux conditions, i.e. the operation is performed in the pressure-independent flux regime under fixed hydrodynamic conditions. Assuming $R_1 = 1$ and $R_2 = 0$, the limiting flux can be expressed as

$$q(c) = k' A \ln \frac{c_{\lim}}{c}, \tag{9}$$

where the constants k', A, and $c_{\lim}$ are the mass transfer coefficient under polarised-layer-controlled conditions, the membrane area, and the limiting concentration at the membrane wall, respectively. The macro-solute concentration c_1 is denoted by c. Different nomenclature and symbols have been in use in the literature for presenting Eq. (9) that is historically referred to as "gel polarisation model". From the point of view of mathematical treatment, it is essentially the same diafiltration problem (provided by Eq. (9)-type formula) that has been the subject of experimental and theoretical investigations by many authors (e.g. in [12, 13, 14, 10, 15]). Note that the model restriction on constant pressure setpoint mentioned in Sect. 2 does not apply here. In fact, pressure may be subject of change as long as the flux is located in the pressure-independent regime, and thus, Eq. (9) holds.

Results. The time-optimal control strategy was found in [10]. Using the results derived in this paper, the optimal concentration curve is defined by (8) and it is a function of the macro-solute only

$$S(c) = q + c\frac{\mathrm{d}q}{\mathrm{d}c} = 0. \tag{10}$$

This shows that optimal operation is obtained at a constant concentration which is from the last equation derived as

$$c = \frac{c_{\mathrm{lim}}}{\mathrm{e}}. \tag{11}$$

This optimal concentration stays on the optimal value if the control is calculated from (7)

$$\alpha(t) = \frac{\frac{\partial S}{\partial c}c}{\frac{\partial S}{\partial c}c} = 1. \tag{12}$$

If the minimum diluant problem is considered, the optimal curve does not exist and optimal operation will consist of concentration step followed by pure dilution.

Here it is implicitly assumed that the actual concentration stays below c_{lim} during the concentration step. If the limit case with $c = c_{\mathrm{lim}}$ is hit, the diluant consumption will be minimised but at infinitely large final time. Therefore, practical considerations indicate that a constraint $c \leq c_{\mathrm{lim}} - \varepsilon$ must be added to the problem formulation where a small positive ε would balance practical duration of the membrane filtration and diluant consumption. This middle stage would thus be characterised by diafiltration operation $\alpha = 1$ at $c = c_{\mathrm{lim}} - \varepsilon$.

4.2. Optimisation at limiting flux with viscosity-dependent mass transfer coefficient

The stagnant film model for $R_1 = 1$ and $R_2 = 0$ is given by

$$q = kA \ln \frac{c_{\mathrm{lim}}}{c}. \tag{13}$$

A thorough discussion on the model parameters and their concentration-dependency can be found in [13, 16]. Let us now consider an application where the filtration performance can be described by a special case of Eq. (13) such that

$$q(c, c_{\mathrm{lim}}) = k(c, c_{\mathrm{lim}})A \ln \frac{c_{\mathrm{lim}}}{c}, \tag{14}$$

where the wall concentration c_{lim} is assumed to be a constant and the mass transfer coefficient k is a function of c and c_{lim}. Note that Eq. (14) can be also seen as a slightly generalised form of Eq. (9). We consider both laminar and turbulent flow

$$k = \begin{cases} k_0 \mathrm{e}^{\gamma z(c - c_{\mathrm{lim}})} & \text{laminar} \\ k_0 \mathrm{e}^{\gamma [z(c - c_{\mathrm{lim}}) - c/2]} & \text{turbulent} \end{cases} \tag{15}$$

where k_0 is average mass transfer coefficient without the wall correction factor, the constant γ quantifies the concentration dependence of the solution viscosity and z is the exponent in the wall correction factor.

Results. The optimal switching curve $S(c)$ for minimum time control is defined from (4.1) as

$$\ln \frac{c_{\mathrm{lim}}}{c} \left(1 + \frac{c}{k} \frac{\mathrm{d}k}{\mathrm{d}c}\right) = 1. \tag{16}$$

Note that it again depends on c only and is a constant.

The appropriate optimal concentration for both types of flow is given from non-linear equation

$$S_{\mathrm{lam}}(c) : \; (c\gamma z + 1) \ln \frac{c_{\mathrm{lim}}}{c} = 1, \tag{17a}$$

$$S_{\mathrm{tur}}(c) : [c\gamma(z - 0.5) + 1] \ln \frac{c_{\mathrm{lim}}}{c} = 1. \tag{17b}$$

These equations predict that the optimum concentration will be shifted to higher concentrations (i.e. higher than $c_{\mathrm{lim}}/\mathrm{e}$) under laminar flow conditions and to lower concentrations under turbulent conditions. Both expressions reduce to the classic result when $\gamma = 0$, i.e., when viscosity effects are negligible.

The minimum diluant operation will be again achieved by concentration step followed by pure dilution.

4.3. Optimisation at fixed pressure with the osmotic pressure model

To show an applicability of the proposed approach we assume the same problem as above where the limiting concentration c_{lim} is for given c defined by an implicit relation

$$E(c, c_{\mathrm{lim}}) = k \ln \frac{c_{\mathrm{lim}}}{c} - \frac{\Delta P - \pi(c_{\mathrm{lim}})}{\mu_0 R_m} = 0. \tag{18}$$

In this model, the flux as predicted by concentration polarisation theory is equated to the flux as predicted by osmotic pressure theory [17]. Function $\pi(c_{\mathrm{lim}})$ is defined experimentally, usually as a third order polynomial with coefficients π_1, π_2, π_3

$$\pi(c_{\mathrm{lim}}) = \pi_1 c_{\mathrm{lim}} + \pi_2 c_{\mathrm{lim}}^2 + \pi_3 c_{\mathrm{lim}}^3. \tag{19}$$

For simplicity, only laminar case will be considered, case for turbulent regime can be derived in the same manner. Therefore, the average mass transfer coefficient can be written as

$$k = k_0 \mathrm{e}^{\gamma z (c - c_{\mathrm{lim}})}. \tag{20}$$

Results. If minimum time operation is considered, the optimal switching curve $S(c)$ will be again a constant defined by (4.1).

To derive the expression for derivative of q with respect to c, let us note that (18) defines an implicit relation between c and c_{lim} and the following holds

$$\frac{\partial c_{\mathrm{lim}}}{\partial c} = -\frac{\frac{\partial E}{\partial c}}{\frac{\partial E}{\partial c_{\mathrm{lim}}}}, \tag{21a}$$

$$\frac{\partial E}{\partial c} = \frac{\partial k}{\partial c}\ln\frac{c_{\mathrm{lim}}}{c} - k\frac{1}{c}, \tag{21b}$$

$$\frac{\partial E}{\partial c_{\mathrm{lim}}} = \frac{\partial k}{\partial c_{\mathrm{lim}}}\ln\frac{c_{\mathrm{lim}}}{c} + k\frac{1}{c_{\mathrm{lim}}} + \frac{1}{\mu_0 R_m}\frac{\partial \pi(c_{\mathrm{lim}})}{\partial c_{\mathrm{lim}}}. \tag{21c}$$

Then, the following holds

$$\frac{\mathrm{d}q}{\mathrm{d}c} = \frac{\partial q}{\partial c} + \frac{\partial q}{\partial c_{\mathrm{lim}}}\frac{\partial c_{\mathrm{lim}}}{\partial c}, \tag{22a}$$

$$\frac{1}{A}\frac{\mathrm{d}q}{\mathrm{d}c} = \frac{\partial k}{\partial c}\ln\frac{c_{\mathrm{lim}}}{c} - \frac{k}{c} + \left(\frac{\partial k}{\partial c_{\mathrm{lim}}}\ln\frac{c_{\mathrm{lim}}}{c} + \frac{k}{c_{\mathrm{lim}}}\right)\frac{\partial c_{\mathrm{lim}}}{\partial c}. \tag{22b}$$

The optimal switching curve $S(c)$ can be derived as

$$0 = \left(\frac{1}{c_{\mathrm{lim}}} - \gamma z \ln\frac{c_{\mathrm{lim}}}{c}\right)\ln\frac{c_{\mathrm{lim}}}{c} + \frac{1}{k}\frac{1}{\mu_0 R_m}\frac{\partial \pi(c_{\mathrm{lim}})}{\partial c_{\mathrm{lim}}}\left(\ln\frac{c_{\mathrm{lim}}}{c}(1+\gamma z c) - 1\right). \tag{23}$$

The optimal concentration c and the corresponding wall concentration c_{lim} can then be calculated from the system of non-linear equations (18) and (23).

Both rejection coefficients are constant again and therefore minimum diluant operation is defined with α being on constraints.

4.4. Case study 1: Separation of lactose from proteins

We consider a process described in [18] where lactose is separated from milk proteins. Both retention coefficients are constant $R_1 = 1$, $R_2 = 0$. We will assume $\alpha \geq 0$ and unbounded from above. Permeate flow was determined experimentally as

$$q(c_1, c_2) = b_0 + b_1 \ln c_1 + b_2 \ln c_2 = 63.42 - 12.439 \ln c_1 - 7.836 \ln c_2, \tag{24}$$

where c_1 is concentration of proteins and c_2 denotes concentration of lactose.

Results. The optimum concentration curve for the minimum time problem depends on both concentrations and is given by (8) as

$$S(c_1, c_2) = b_0 + b_1 + b_2 + b_1 \ln c_1 + b_2 \ln c_2 = 0. \tag{25}$$

Once these optimal concentrations are obtained the control is calculated from (7)

$$\alpha(t) = \frac{\frac{\partial S}{\partial c_1}c_1}{\frac{\partial S}{\partial c_1}c_1 + \frac{\partial S}{\partial c_2}c_2} = \frac{b_1}{b_1 + b_2}. \tag{26}$$

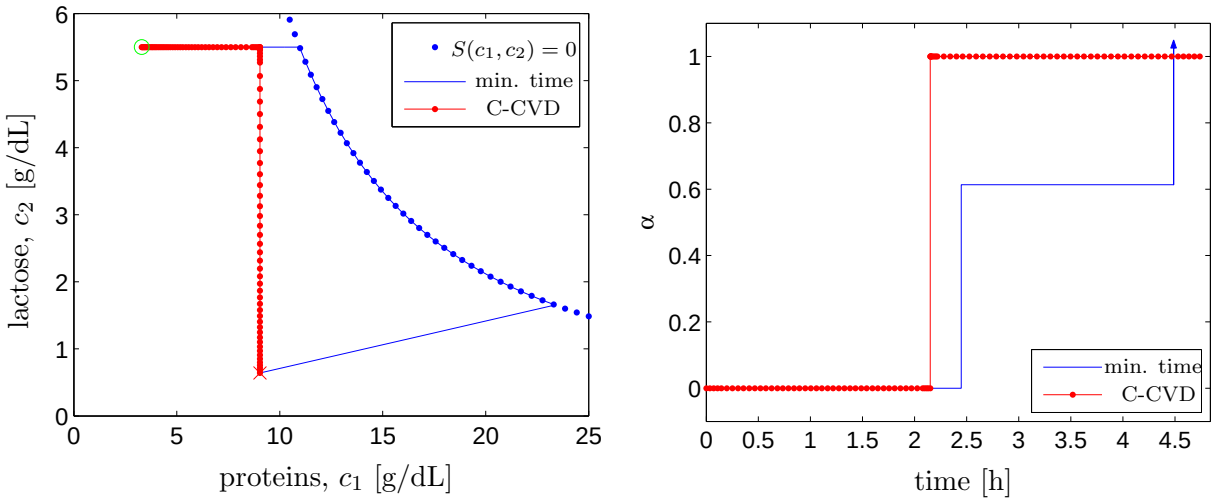

Figure 3: Separation of lactose from proteins: comparison of minimum time and C-CVD control strategy in concentration diagram (left plot) and corresponding control (right plot).

As we can see, even if the optimal concentration curve depends on both concentrations, the corresponding optimal control is constant and less than one due to special expression for q.

We consider to drive concentrations from initial point $[c_{1,0}, c_{2,0}] = [3.3, 5.5]$ to final point $[c_{1,\mathrm{f}}, c_{2,\mathrm{f}}] = [9.04, 0.64]$. To perform this task in minimum time we use a three step strategy (see state diagram in Fig. 3):

1. Start at circle, horizontal line: pure ultrafiltration until we arrive at optimal surface $S(c_1, c_2) = 0$.
2. Stay on this surface using constant control $\alpha = b_1/(b_1 + b_2) = 0.61$ until the concentration ratio is the same as the final one: $c_1(t)/c_2(t) = c_{1,\mathrm{f}}/c_{2,\mathrm{f}}$.
3. Follow the line towards origin: use pure dilution step to arrive at the final point (cross).

We note that the final dilution step with $\alpha = \infty$ need not occur in the filtration setup. The solution can be treated in some separate equipment after the actual filtration operation. Therefore, we can interpret its duration as zero and it does not add to the overall processing time. However, if the dilution step is not realistic we can replace $\alpha = \infty$ with some upper limit $\alpha = \alpha_{\max}$. Overall structure of optimal control will remain the same, only the cost function value will increase correspondingly.

The resulting final time in this case is 4.49 hours. This can be compared to the operation described in [18] where two step process C-CVD (UF-CVD) was used. This traditional operation takes for the same initial and final conditions 4.74 hours, an increase of 5.6%. As we can see from the right diagram in Fig. 3, traditional CVD step ($\alpha = 1$) starts earlier but it takes more time to reach the final point as the VVD step ($\alpha = 0.61$) in minimum time control. There, it is assumed that the last step (upward arrow) takes no time.

The overall minimum time strategy is sketched in Fig. 4 where horizontal solid lines represent evolution of concentrations during the concentration (UF) step and dashed lines

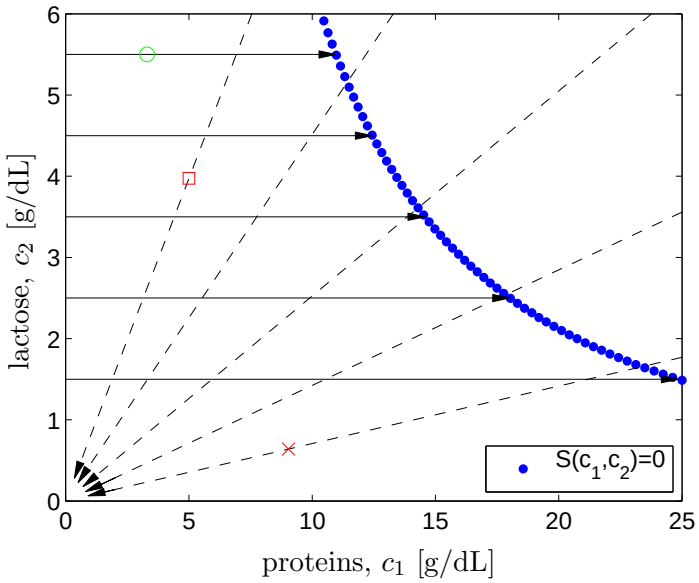

Figure 4: Separation of lactose from proteins: analytical minimum time control in concentration diagram.

during pure dilution ($\alpha = \infty$). Arrows in these lines denote directions, in which the respective operations influence concentrations. Previously used initial and final points are depicted again to illustrate how the minimum time optimal strategy is chosen. We note that it seems theoretically possible to use two step strategy starting with dilution step followed by ultrafiltration. However, the resulting final time will be much longer. As a practical rule of thumb it is necessary to consider only such strategies that approach the optimal concentration curve. Also note that it is not possible to use dilution and ultrafiltration steps more times. Optimal control theory does not allow this arbitrary switching and the resulting trajectory can consists at most of three steps.

Consider now a case where we want to arrive at final point $[5, 3.97]$ (square in Fig. 4) starting from the same initial point. As shown in Fig. 4, it is not admissible to use three step operation since once we would reach the surface $S(c_1, c_2)$ (by using UF) it would not be possible anymore to reach the final point neither by using UF nor pure dilution. Thus, the middle step is skipped in this case and minimum time operation is attained only by using ultrafitration and pure dilution operation. Order of these operations is again not arbitrary and it is such that the resulting curve in state diagram is as close as possible to optimal surface $S(c_1, c_2)$. The switching moment between the steps is determined by the concentration ratio equal to $c_{1,\mathrm{f}}/c_{2,\mathrm{f}}$.

The optimal concentration surface does not exist for the minimum diluant problem and the resulting optimal operation is of bang-bang type. To illustrate this we could construct a diagram similar to Fig. 4 by prolonging the horizontal lines corresponding to pure ultrafiltration.

4.5. Case study 2: Albumin – ethanol separation

This ultrafiltration/diafiltration process was originally studied in [5]. The flow q was determined experimentally as

$$q(c_1, c_2) = \frac{1}{b_1 + b_2 c_1 + b_3 c_2 + b_4 c_1 c_2 + b_5 c_1^2 + b_6 c_2^2}, \tag{27}$$

where b_i are constants that can be found in [5]. Both retention coefficients are constant $R_1 = 1$, $R_2 = 0$ and $\alpha \in [0, 1]$.

We studied optimal control of this diafiltration process by means of numerical methods in [11]. Here we compare proposed analytical procedure with numerical results from [11]. Three different cases of initial concentration of ethanol $c_{2,0}$ are investigated: case 1 with $98.35\,\mathrm{kg\,m^{-3}}$, case 2 with $146.3\,\mathrm{kg\,m^{-3}}$, and case 3 with $194.3\,\mathrm{kg\,m^{-3}}$. Other concentrations are held constant: $c_{1,0} = 15\,\mathrm{kg\,m^{-3}}$, $c_{1,\mathrm{f}} = 80\,\mathrm{kg\,m^{-3}}$, $c_{2,\mathrm{f}} = 0.1\,\mathrm{kg\,m^{-3}}$.

Results. The optimum concentration curve for the minimum time problem depends on both concentrations and is given by (8) as

$$S(c_1, c_2) = b_1 - b_5 c_1^2 - c_1 c_2 b_4 - b_6 c_2^2 = 0. \tag{28}$$

Once these optimal concentrations are obtained the control is calculated from (7)

$$\alpha(t) = \frac{\frac{\partial S}{\partial c_1} c_1}{\frac{\partial S}{\partial c_1} c_1 + \frac{\partial S}{\partial c_2} c_2} = \frac{0.5 b_4 c_1 c_2 + b_5 c_1^2}{b_5 c_1^2 + b_4 c_1 c_2 + b_6 c_2^2}. \tag{29}$$

Figures 5 and 6 show the optimal control of diafiltration process for cases 1 and 2. Even if analytical and numerical curves seem to be different, the resulting final times are practically the same.

Both initial and final concentrations in case 1 are below the optimal concentration curve. Therefore, the corresponding optimal operation is to perform UF first until the optimal curve is attained. In the second step, α is given by (29) until the final concentration of albumin $c_{1,\mathrm{f}} = 80\,\mathrm{kg\,m^{-3}}$ is reached. The final step is CVD until the final concentration of ethanol is reached.

Cases 2 and 3 differ from the case 1 as they start above the optimal concentration curve. Therefore, the first step is CVD (upper constraint on α is 1). Its duration depends on the distance of the initial point from the optimal curve. The second and the third steps are then the same as before.

Table 1 gives a comparison and optimality loss of C-CVD (UF followed by CVD) and VVD control strategy. VVD strategy is clearly suboptimal. We can observe that C-CVD strategy is nearly time-optimal even if the minimum time control is quite different from that used in C-CVD. This results from the restriction on upper value of control α. If this value is raised such that pure dilution step is allowed the resulting operation times will dramatically drop down.

In the case of minimum diluant problem, bang-bang type of control (CVD operation) was observed numerically in [11]. Results derived here confirm this behaviour as both retention coefficients are constant. Comparison with VVD strategy shows 61% optimality loss in all considered cases.

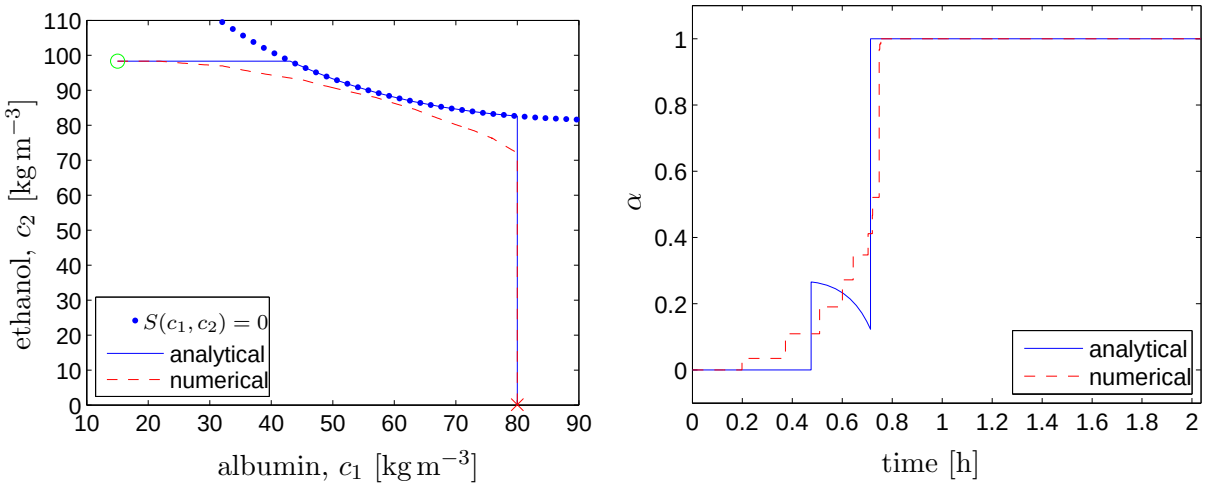

Figure 5: Analytical and numerical [11] minimum time control for Case 1. Left plot – optimal concentrations diagram, right plot – optimal $\alpha(t)$.

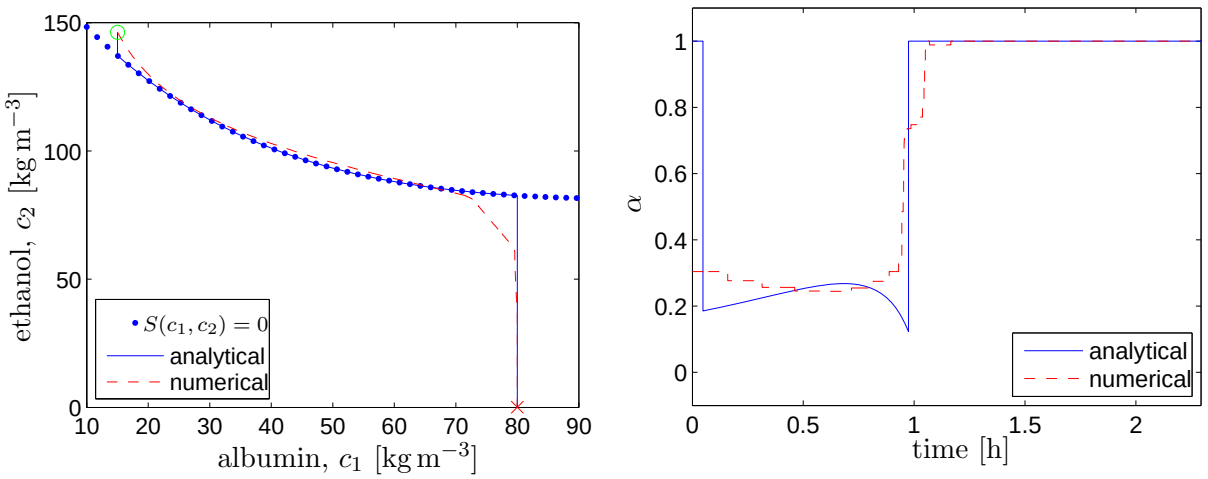

Figure 6: Analytical and numerical [11] minimum time control for Case 2. Left plot – optimal concentrations diagram, right plot – optimal $\alpha(t)$.

Table 1: Comparison of time optimality loss (Δ) between optimal control and traditionally used strategies.

	Case 1	Case 2	Case 3
C-CVD	0%	0.9%	0.4%
VVD	15%	13%	11%

Table 2: Design factors and their levels (adopted from [19]).

Factor	Code	Unit	Factor levels	
			Low(-)	High(+)
Pressure	A	bar	4	8
Temperature	B	°C	28	50
pH	C	-	4	11
Dye concentration	D	ppm	100	400
Salt concentration	E	ppm	1000	6000

4.6. Case study 3: Dye – salt separation

We consider the nanofiltration (NF) model reported by Lau and Ismail [19]. In their study, response surface methodology (RSM) was employed to evaluate the separation performance of an NF membrane in the removal of salt and reactive dye by varying different variables such as pressure, temperature, pH, dye concentration and salt concentration. According to half fractional design of experiments (DoE), twenty-nine experiments were carried out to investigate the effect of five inputs (i.e. pressure, temperature, pH, dye concentration, and salt concentration) on three responses (i.e. permeate flux, dye rejection, and salt rejection). The design factors and their levels are shown in Table 2. The permeation of salt was found to be greatly influenced by pressure, pH and salt concentration whereas the rejection of dye remained constant regardless of the changes in the variables. The mean value of the dye rejection for the entire experimental data set is 98.0%. The resulting surface responses for the salt rejection and the permeate flux in terms of coded factors are given as

$$Y_1 = 83.26 + 2.79A + 8.37C - 4.52E - 1.96AC, \tag{30a}$$

$$Y_3 = 6.31 \cdot 10^{-7} + 1.89 \cdot 10^{-7}A - 1.67 \cdot 10^{-8}D - 1.30 \cdot 10^{-7}E - \\ - 6.07 \cdot 10^{-8}C^2 - 2.85 \cdot 10^{-8}AE - 2.096.31 \cdot 10^{-8}BD, \tag{30b}$$

where Y_1 is the salt rejection expressed in percentage and Y_3 is the permeate flux given in $\mathrm{m\,s^{-1}}$.

In this case study, we consider a textile waste stream with the initial dye and salt concentrations to be $c_1(0) = 100\,\mathrm{ppm}$ and $c_2(0) = 4000\,\mathrm{ppm}$. This is to be processed to meet the quality constraints of the final product, $c_1(t_\mathrm{f}) = 400\,\mathrm{ppm}$ and $c_2(t_\mathrm{f}) = 1000\,\mathrm{ppm}$.

Lau and Ismail [19] have found that the salt rejection increases with pressure and decreases with feed pH. Thus, we fix the pressure at 4 bar, the pH at 4, and additionally, the temperature at 50°C. Using original scale instead of the coded factors and taking into account the above mentioned process conditions, the membrane response can be formulated as follows

$$R_1 = b_1, \tag{31a}$$

$$R_2(c_2) = b_2 - b_3c_2, \tag{31b}$$

$$q(c_1, c_2) = b_4 - b_5c_1 - b_6c_2, \tag{31c}$$

Table 3: Model parameters.

constant	value
b_1	0.9800
b_2	0.7647
b_3	1.8080×10^{-5}
b_4	5.8607×10^{-7}
b_5	2.5066×10^{-10}
b_6	4.0600×10^{-11}

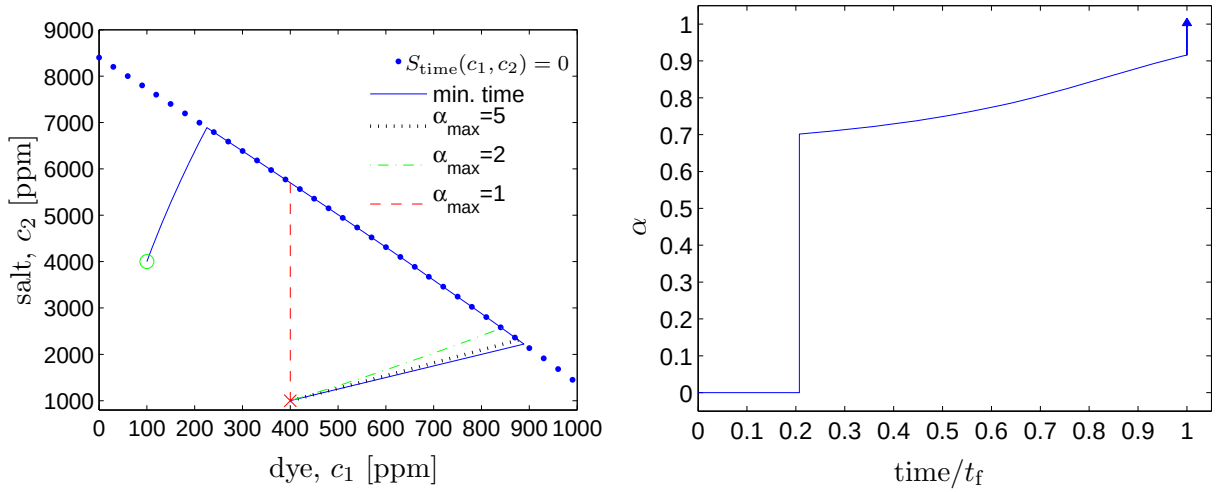

Figure 7: Dye – salt separation: optimal operation. Left plot – optimal concentrations diagram with different values of $\alpha_{\max}$, right plot – optimal $\alpha(t)$.

where b_i are constants that are listed in Table 3.

Results. The dye rejection R_1 is independent of the feed composition and we can assume that it is sufficiently close to unity. In this case, because $R_{11} = R_{12} = 0$ and $R_1 \approx 1$, the minimum time state curve is given by (5). Using the membrane response formulas given in (31b) and (31c) we then obtain

$$S_{\text{time}}(c_1, c_2) = (b_3c_2 - b_2 + 1)\,(2b_5c_1 - b_4 + 2b_6c_2) + b_3c_2\,(b_5c_1 - b_4 + b_6c_2) = 0. \tag{32}$$

The singular control $\alpha(t)$ is calculated by (7) which results in

$$\begin{aligned}\alpha(t) = &\frac{c_2\,(2b_2b_6 - 2b_2^2b_6 - 2b_2b_3b_4) + c_2^2\,(2b_3^2b_4 - 2b_3b_6 + 8b_2b_3b_6) - 6b_3^2b_6c_2^3}{2(b_5c_1 + b_6c_2 - b_2b_5c_1 - b_3b_4c_2 - b_2b_6c_2 + 3b_3b_6c_2^2 + 3b_3b_5c_1c_2)}\\ &+ \frac{c_1\,(2b_1b_5 - 2b_1b_2b_5) + c_1c_2\,(3b_1b_3b_5 + 3b_2b_3b_5) - 3b_3^2b_5c_1c_2^2}{2(b_5c_1 + b_6c_2 - b_2b_5c_1 - b_3b_4c_2 - b_2b_6c_2 + 3b_3b_6c_2^2 + 3b_3b_5c_1c_2)}.\end{aligned} \tag{33}$$

The optimal control is shown in Fig. 7. Both initial and final concentrations are located under the optimal concentration curve and the optimal process is a three-step process. The first step is concentration mode ($\alpha = 0$) until optimum concentration curve presented

Table 4: Comparison of time optimality loss (Δ) between optimal control, optimal control with different $\alpha_{\max}$ and traditionally used strategies.

control strategy	C-DVD ($\alpha_{\max}$=5)	C-DVD ($\alpha_{\max}$=2)	C-DVD ($\alpha_{\max}$=1)	C-CVD	VVD
Δ	0.1%	0.6%	8.3%	14.0%	55.3%

by (32) is reached. The second step is a dynamic-volume diafiltration with non-constant $\alpha(t)$ where the diluant usage is given by (33). Since there is no upper limit for α, the third step is a pure dilution mode with $\alpha = \infty$. This step starts when the concentration ratio is the same as the final one: $c_1(t)/c_2(t) = 0.4$.

Figure 7 shows for comparison the concentration profiles for different choice of maximum value of α. As noted above, the limiting cast $\alpha = \infty$ can simply be realized by postponing the pure dilution step after the end of batch processing once the final solution is prepared for the next operation. Another possibility would be to constrain $\alpha_{\max} \approx 5$ where the difference to optimal operation is not large.

Table 4 shows comparison of time optimality loss between optimal control ($\alpha_{\max} = \infty$), optimal control with $\alpha_{\max}$ restricted to different values and traditional control approaches. Here we can see that the difference between optimal control and optimal control with $\alpha_{\max} = 5$ is practically negligible. This difference increases, but not dramatically, if α is constrained from above by 2. However, it becomes significant (8.3% of optimality loss) in the case of $\alpha_{\max} = 1$. Comparison with traditional control strategies shows 14% slower process with C-CVD approach. Finally, the VVD approach controls the process slower by more than 50%.

Also note that traditional operation is constrained with $c_1 < 400\,\text{ppm}$ whereas the proposed optimal operation needs this constraint approximately twice as large. It may happen that $S(c_1, c_2)$ is located outside of the experimentally investigated region of c_1 and c_2 where the membrane response model is not validated. It seems that the common practice is that investigators focus on obtaining experimental data from the design space bounded by ($c_{1,0}$, $c_{2,0}$) and ($c_{1,\text{f}}$, $c_{2,\text{f}}$) coordinates whereas optimal operation might be performed outside of this area. In other words, optimal operation might involve over-concentration or dilution of the solution and thus, a bigger design space should be considered during the experimentation phase.

Recalling that $R_1 = 1$ is assumed, the optimal state curve for the minimum diluant problem is defined by (6). Using the membrane response formulas given in (31b) and (31c), the optimal state curve can be written as

$$S_{\text{diluant}}(c_2) = b_2 - 2b_3c_2 - 1 = 0. \tag{34}$$

This results in a single equation involving only variable c_2. Solving this equation yields a negative value ($c_2 = -6508$) that is technically not feasible. The optimal control is then of bang-bang type: a two-step process where the first step is a concentration step with $\alpha = 0$ and the second is a dilution mode operation applying the maximum value of α.

4.7. Case study 4: Sucrose – sodium chloride separation

This case study is taken from our previous study [7] where we concentrated on utilisation of numerical methods of dynamic optimisation to derive the optimal control of diafiltration process using an economic cost function.

This case study represents diafiltration system with one variable retention coefficient (R_1 is almost constant and equal to one) and the empirical relations for q and R_2 as functions of feed composition are as follows:

$$q = U_1(c_2)\mathrm{e}^{U_2(c_2)c_1}, \tag{35a}$$

$$R_2 = V_1(c_2)\mathrm{e}^{V_2(c_2)c_1}, \tag{35b}$$

where U_1, U_2, V_1, and V_2 are second order polynomials in c_2 whose coefficients were determined from laboratory experiments with the process solution [20]. It is assumed that $\alpha \in [0, 1]$.

Results. It is desired to concentrate sucrose and dilute sodium chloride in solution from their initial concentrations given by point $[c_{1,0}, c_{2,0}] = [10, 250]$ to final concentrations represented by the point $[c_{1,\mathrm{f}}, c_{2,\mathrm{f}}] = [50, 50]$.

The optimum concentration curve for the minimum time problem depends on both concentrations and is given by (5). The optimum concentration curve corresponding to the minimum diluant problem is given by (6).

Both curves have been found using numerical non-linear equation solvers. Figure 8 shows the optimal control of the process for the considered case. Results show that even if the optimal concentration curve expressions look entirely different, solutions to both optimal control problems are nearly the same: minimum-time approach takes 10.24 hours and 0.143 m^3 of diluant, and minimum-diluant approach takes 10.25 hours and consumes 0.143 m^3 of diluant. In contrast to that, a traditional treatment with NF followed by CVD and ended by another NF (C-CVD-C) step lasts 14.46 hours and uses 0.256 m^3 of diluant. Here 3.61 and 1.35 are pre-concentration and post-concentration factors, respectively.

Although the two-step approach ($\alpha = \{0, 1\}$) would result in faster process, it would yield high concentrations of salt during the process run that lay out of the range studied in [20]. The model is not validated through experiments for this regime, thus, we have to exclude this strategy from further discussion. In general, a great care is needed when using empirical models, especially polynomials, for predicting flux and rejections out of the validated range. In such cases, application of mechanism-driven models could be considered instead. Note that even complex physical models can be easily treated by the here proposed optimisation methodology. Physical models can be used first to compute membrane response for a defined set of c_1 and c_2 that covers the entire area of question, and then simplified by fitting some simpler empirical relations.

VVD approach is clearly sub-optimal since it takes 22.753 hours and 0.505 m^3 of diluant. Another interesting result here is that C-VVD (process duration 14.07 hours, diluant consumption 0.253 m^3, pre-concentration factor 3.69) approach is faster than C-CVD-C.

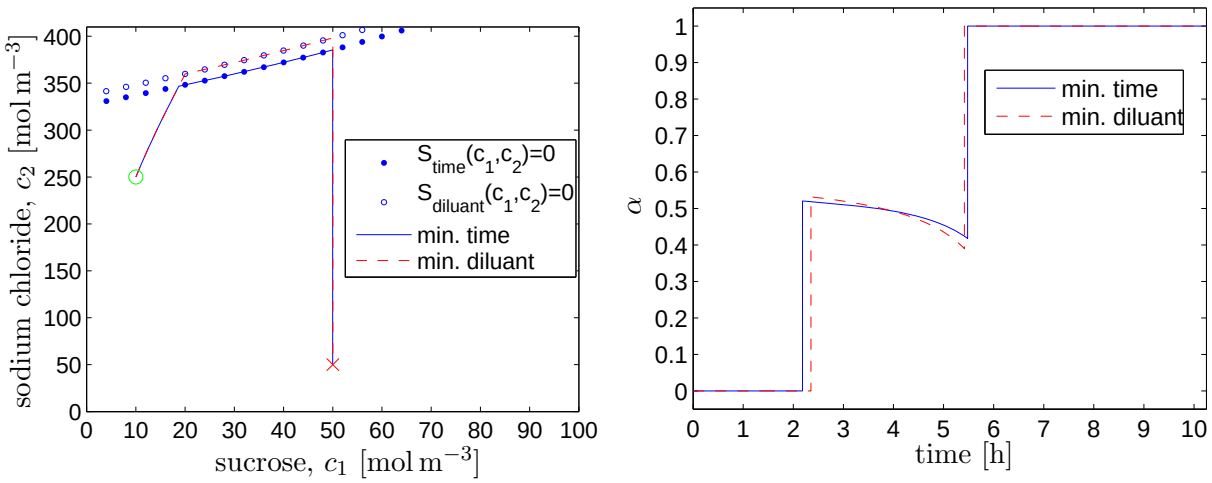

Figure 8: Analytical optimal control of sucrose–sodium chloride separation. Left plot – optimal concentrations diagram, right plot – optimal $\alpha(t)$.

Table 5: Comparison of optimality loss (Δ) between optimal control and traditionally used strategies.

	Δ_{time}	Δ_{diluant}
C-CVD-C	41%	79%
C-VVD	37%	77%
VVD	122%	253%

However, this is caused by the previously mentioned inadmissibility of two-step C-CVD operation. Table 5 summarizes how much we gain by using of optimal control in comparison with traditional strategies.

4.8. Case study 5: Radiopaque – ethylene glycol separation

We treat a variation of the case study examined in [9] where authors studied filtration using reverse osmosis membrane to treat a solution containing 12 g/dL of radiopaque component (c_1) and 0.5 g/dL of ethylene glycol (c_2) to end up with the product with concentrations: 40 g/dL of radiopaque and 0.01 d/dL of ethylene glycol. For the purpose of this study constants which characterize rejection of radiopaque were slightly changed to reflect the situation where rejection R_1 is not close to one. Model of the membrane response then reads as

$$q = -29.19 \ln c_1 + 118.1, \tag{36a}$$
$$R_1 = 1 - (0.01c_1 + 0.25c_2 + 0.1), \tag{36b}$$
$$R_2 = 1 - (0.0073c_1 + 0.813). \tag{36c}$$

Results. This example represents a situation when we are not able to obtain expression for optimal concentration surface analytically. We proceed as suggested in Section 3.2 and derive an expression for singular optimal control from (A.22). Then we use numerical

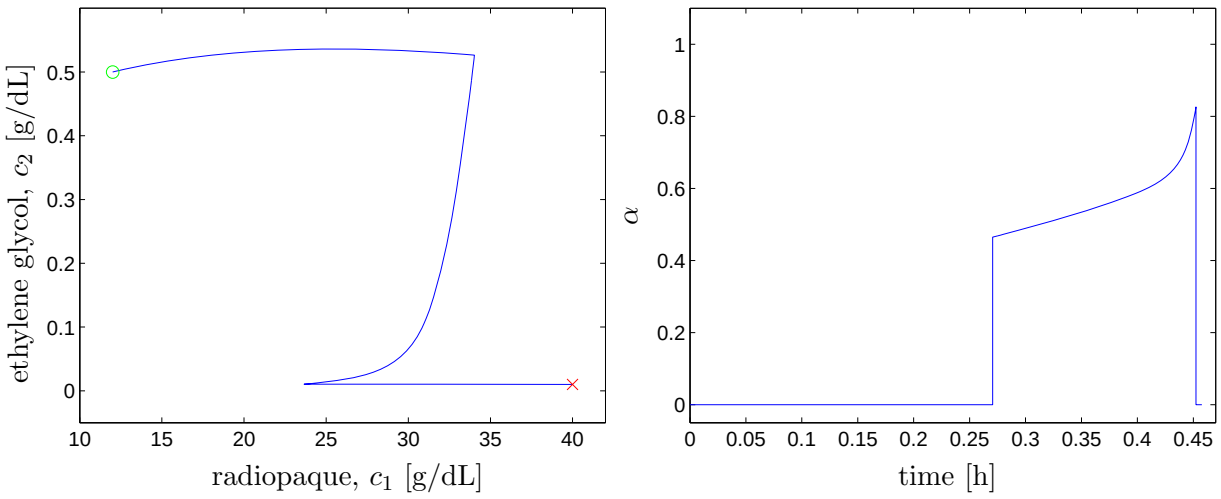

Figure 9: Minimum time control of radiopaque – ethylene glycol separation.

optimization to find corresponding lengths of three time intervals and extremal values of α in the first and third phases.

Once the structure and lengths of respective intervals are fixed, we can operate the process optimally with singular control (A.22) in the middle part.

Fig. 9 shows optimal evolution of concentrations under minimum time control α. When compared with traditional control strategies, minimum time strategy saves 4.5% of process time in comparison with C-CVD (CVD step done at concentration c_{lim}/e) and 18% of process time when compared to VVD control strategy.

In minimum diluant case, although that it is possible that optimal surface exists, it did not appear for given initial and final conditions. The optimal control is of bang-bang type.

5. Conclusions

This study deals with batch concentration/diafiltration problems that are often occur in the RO, NF, UF, and MF engineering practice. We have employed optimal control theory and derived an analytical solution to the problem that involves complete rejection of macro-solute ($R_1 = 1$), concentration-dependent rejection of micro-solute ($R_2 = R_2(c_1, c_2)$), and a general flux model ($q = q(c_1, c_2)$). The extension of this problem to concentration-dependent rejection of macro-solute ($R_1 = R_1(c_1, c_2)$) remains analytically unsolved. However, for this general case we have developed an efficient numerical procedure that exploits the findings of our theoretical analysis and considerably reduces the required computational efforts.

We provide a step-by-step procedure to compute the optimal diluant utilization. By applying this procedure, one can determine the optimal time-varying profile of wash-water addition for the entire operation. In some cases, the computed optimal profile is found to be a sequence of conventionally-used steps (i.e. concentration mode, constant-volume diafiltration, variable-volume diafiltration). The provided procedure readily finds the optimal sequence (number and order) of such steps as well as the corresponding switching times.

In most of the cases, however, the optimal trajectory does not follow the shape of known diafiltration techniques. Such non-linear α-control strategies can either be implemented through advanced control configuration or be simplified by a sequence of conventional process steps having a similar shape. The procedure allows one to quantify time and diluant savings of the optimal trajectory, thus, it is a useful engineering tool in the decision maker's hand.

We have demonstrated through selected case studies how one can apply the provided optimization theory. We have considered various, both theoretical and empirical, membrane response models as inputs for the given optimization procedure. A great deal of care is needed when generalizing the findings as far as general patterns in the shape of optimal trajectory are considered among different applications. This is due to the great variety and complexity of possible membrane response models regarding concentration-dependent rejections and flux functions. Note that the provided procedure is general in a sense that it can be readily applied to different membrane response models, but the computed optimal profile may vary with the complexity of the membrane response model, the initial and final values, and the constraints involved in the model. We have shown that in many cases, time and diluant savings become more significant with increasing complexity of the model of membrane response, e.g. strongly non-linear membrane response with regard to both considered components.

Analysis and numerical optimisation have shown that the optimal solution of the time minimisation problem consists of usually three stages. The first and the last ones take extremal values of α which is pure concentration and either pure dilution (when α is unbounded from above) or operation with maximal α. The middle stage can have various time varying trajectories of control. Its complexity depends in the majority of studied cases on the functional dependence of the outflow q on concentrations. Often, if it is a function of macro-solute concentration only, the corresponding middle control strategy is constant macro-solute concentration maintaining operation (this is CVD if $R_1 = 1$) with various optimal concentrations of the macro-solute. This is shown in the examples with limiting flux and osmotic pressure models. There are also cases where the middle stage is VVD with $\alpha < 1$ as can be seen in the first treated case study. The most general form, however, is a complex non-linear curve (remaining case studies).

The problem of the minimisation of the diluant consumption is analogous to the preceding case, but it depends only on the functional dependence of rejection coefficients on concentrations. The most usual case of constant rejection coefficients results in the so-called bang-bang control where only UF and pure dilution are allowed.

Results indicate that improvement of the proposed procedure as compared to traditional operation depends on the problem complexity. Processes with simpler membrane and/or permeate flow characteristics already operate near optimal regime. The improvement for more complex scenarios can be significant enough to invest in better models and advanced control configuration.

List of symbols

A	membrane area (m^2)
c	concentration in feed tank
H	Hamiltonian function
J	objective function
k	mass transfer coefficient ($\mathrm{m\,s}^{-1}$)
k_0	mass transfer coefficient without the wall correction factor ($\mathrm{m\,s}^{-1}$)
k'	mass transfer coefficient under limiting flux conditions ($\mathrm{m\,s}^{-1}$)
ΔP	average transmembrane pressure (Pa)
q	permeate flow ($\mathrm{m}^3\,\mathrm{s}^{-1}$)
R	rejection coefficient
R_m	membrane resistance (m^{-1})
S	optimal state surface
t	operation time (s)
$\boldsymbol{u}$	vector of control variables
V	volume in feed tank (m^3)
$\boldsymbol{x}$	vector of state variables
z	exponent in the wall correction factor in Eq. (15)

Greek symbols

α	proportionality factor of diluant flow to permeate flow
γ	coefficient in Eq. (15)
$\boldsymbol{\lambda}$	vector of adjoint variables
μ_0	solution viscosity (Pa s)
π	osmotic pressure (Pa)

Subscripts

i	component (i=1 macro-solute, and i=2 micro-solute)
0	initial condition
f	final condition
lim	limiting

Abbreviations

C	concentration mode
CVD	constant-volume diafiltration
DF	diafiltration
DVD	dynamic-volume diafiltration
MF	microfiltration
NF	nanofiltration
RO	reverse osmosis
UF	ultrafiltration
VVD	variable-volume diafiltration
VCF	volume concentration factor

Acknowledgements

This research is a cooperative effort. The first and the second author acknowledge the contribution of the Scientific Grant Agency of the Slovak Republic under the grants 1/0537/10, 1/0095/11. The fourth author would like to thank the Hessen State Ministry of Higher Education, Research and the Arts for the financial support within the Hessen initiative for scientific and economic excellence (LOEWE-Program).

[1] A.-S. Jönsson, G. Trägårdh, Ultrafiltration applications, Desalination 77 (1990) 135 – 179, Proceedings of the Symposium on Membrane Technology. doi:10.1016/0011-9164(90)85024-5.

[2] F. Lipnizki, J. Boelsmand, R. F. Madsen, Concepts of industrial-scale diafiltration systems, Desalination 144 (1-3) (2002) 179 – 184. doi:10.1016/S0011-9164(02)00309-0.

[3] B. Maiorella, G. Dorin, A. Carion, D. Harano, Crossflow microfiltration of animal cells, Biotechnology and Bioengineering 37 (2) (1991) 121–126. doi:10.1002/bit.260370205.

[4] R. van Reis, E. M. Goodrich, C. L. Yson, L. N. Frautschy, R. Whiteley, A. L. Zydney, Constant C_{wall} ultrafiltration process control, Journal of Membrane Science 130 (1-2) (1997) 123–140.

[5] M. Jaffrin, J. Charrier, Optimization of ultrafiltration and diafiltration processes for albumin production, Journal of Membrane Science 97 (1994) 71–81.

[6] G. Foley, Ultrafiltration with variable volume diafiltration: A novel approach to water saving in diafiltration processes, Desalination 199 (1-3) (2006) 220–221.

[7] M. Fikar, Z. Kovács, P. Czermak, Dynamic optimization of batch diafiltration processes, Journal of Membrane Science 355 (1-2) (2010) 168–174. doi:10.1016/j.memsci.2010.03.019.

[8] R. Madsen, Design of sanitary and sterile UF and diafiltration plants, Separation and Purification Technology 22-23 (0) (2001) 79 – 87. doi:10.1016/S1383-5866(00)00144-1.

[9] H. Lutz, Membrane filtration with optimized addition of second liquid to maximize flux, United States Patent 5597486, assignee: Millipore Investment Holdings Limited (Wilmington, DE, US) (Jan. 1997).

[10] R. Paulen, G. Foley, M. Fikar, Z. Kovács, P. Czermak, Minimizing the process time for ultrafiltration/diafiltration under gel polarization conditions, Journal of Membrane Science 380 (1-2) (2011) 148–154. doi:10.1016/j.memsci.2011.06.044.

[11] R. Paulen, M. Fikar, Z. Kovács, P. Czermak, Process optimization of diafiltration with time-dependent water adding for albumin production, Chemical Engineering and Processing: Process Intensification 50 (8) (2011) 815–821. doi:10.1016/j.cep.2011.05.010.

[12] P. Ng, J. Lundblad, G. Mitra, Optimization of solute separation by diafiltration, Separation Science and Technology 11 (5) (1976) 499–502.

[13] A. L. Zydney, Stagnant film model for concentration polarization in membrane systems, Journal of Membrane Science 130 (1-2) (1997) 275–281.

[14] M. Yazdanshenas, A. Tabatabaeenezhad, R. Roostaazad, A. Khoshfetrat, Full scale analysis of apple juice ultrafiltration and optimization of diafiltration, Separation and Purification Technology 47 (1–2) (2005) 52–57.

[15] R. Field, Diafiltration under condition of quasi-constant membrane surface concentration, Journal of Membrane Science 383 (1-2) (2011) 301 – 302. doi:10.1016/j.memsci.2011.08.045.

[16] G. Foley, J. Garcia, Ultrafiltration flux theory based on viscosity and osmotic effects: application to diafiltration optimisation, Journal of Membrane Science 176 (1) (2000) 55 – 61. doi:10.1016/S0376-7388(00)00429-4.

[17] J. Howell, R. Field, D. Wu, Ultrafiltration of high viscosity solutions: theoretical developments and experimental findings, Chem. Eng. Sci. 51 (1996) 1405–1415.

[18] N. Rajagopalan, M. Cheryan, Process optimization in ultrafiltration: Flux-time considerations in the purification of macromolecules, Chem. Eng. Comm. 106 (1) (1991) 57–69.

[19] W. J. Lau, A. F. Ismail, Application of response surface methodology in pes/speek blend NF membrane for dyeing solution treatment, Membrane Water Treatment 1 (1) (2010) 49–60.

[20] Z. Kovács, M. Discacciati, W. Samhaber, Modeling of batch and semi-batch membrane filtration processes, Journal of Membrane Science 327 (2009) 164–173.

[21] L. S. Pontryagin, V. G. Boltyanskii, R. V. Gamkrelidze, E. F. Mishchenko, The Mathematical Theory of Optimal Processes, John Wiley & Sons, Inc., New York, 1962.

[22] A. E. Bryson, Jr., Y. C. Ho, Applied Optimal Control, Hemisphere Publishing Corporation, 1975.

[23] C. D. Johnson, J. E. Gibson, Singular solutions in problems of optimal control, IEEE Trans. Automatic Control 8 (1) (1963) 4–15.

[24] B. Srinivasan, S. Palanki, D. Bonvin, Dynamic optimization of batch processes: I. Characterization of the nominal solution, Computers & Chemical Engineering 27 (1) (2003) 1–26.

Appendix A. General formulation of optimal diluant utilization strategy

To solve the specified problems, we will make use of Pontryagin's minimum principle, which is in our case as follows [21, 22].

Let us consider a dynamical system with state vector $\boldsymbol{x} = (c_1, c_2, V)^T$ and scalar control α that enters system equations linearly such that

$$\dot{\boldsymbol{x}} = \boldsymbol{f}(\boldsymbol{x}) + \boldsymbol{g}(\boldsymbol{x})\alpha, \quad \boldsymbol{x}(0) = \boldsymbol{x}_0, \quad \boldsymbol{x}(t_\mathrm{f}) = \boldsymbol{x}_\mathrm{f}, \quad \alpha(t) \in [\alpha_\mathrm{min}, \alpha_\mathrm{max}], \quad t \in [0, t_\mathrm{f}], \tag{A.1}$$

and the cost function

$$J = \min_\alpha \int_0^{t_\mathrm{f}} [F_0(\boldsymbol{x}) + F_\alpha(\boldsymbol{x})\alpha] \,\mathrm{d}t. \tag{A.2}$$

Further, let us define the Hamiltonian H and the vector of adjoint variables $\boldsymbol{\lambda} = (\lambda_1, \lambda_2, \lambda_3)^T$ such that

$$H(\boldsymbol{x}, \alpha, \boldsymbol{\lambda}) = F_0(\boldsymbol{x}) + F_\alpha(\boldsymbol{x})\alpha + \boldsymbol{\lambda}^T [\boldsymbol{f}(\boldsymbol{x}) + \boldsymbol{g}(\boldsymbol{x})\alpha] = H_0(\boldsymbol{x}, \boldsymbol{\lambda}) + H_\alpha(\boldsymbol{x}, \boldsymbol{\lambda})\alpha. \tag{A.3}$$

Necessary conditions of optimality as derived in Pontryagin's principle of minimum are then defined as

$$\alpha = \arg\min_\alpha H(\boldsymbol{x}, \alpha, \boldsymbol{\lambda}), \quad \alpha \in [\alpha_\mathrm{min}, \alpha_\mathrm{max}], \tag{A.4a}$$

$$\dot{\boldsymbol{x}} = \frac{\partial H}{\partial \boldsymbol{\lambda}}, \quad \boldsymbol{x}(0) = \boldsymbol{x}_0, \quad \boldsymbol{x}(t_\mathrm{f}) = \boldsymbol{x}_\mathrm{f}, \tag{A.4b}$$

$$\dot{\boldsymbol{\lambda}} = -\frac{\partial H}{\partial \boldsymbol{x}}, \tag{A.4c}$$

$$H = 0, \quad \forall t \in [0, t_\mathrm{f}]. \tag{A.4d}$$

The last condition arises because of the synergy of two facts: optimal Hamiltonian is constant over the whole time horizon since it is not an explicit function of time and it is zero at final time since the final time is unspecified in treated optimization problems.

The Hamiltonian is linear in α. Thus, its minimum will be attained with α on its boundaries as

$$\alpha = \begin{cases} \alpha_\mathrm{min} & \text{if } H_\alpha > 0, \\ \alpha_\mathrm{max} & \text{if } H_\alpha < 0. \end{cases} \tag{A.5}$$

If $H_\alpha = 0$ the Hamiltonian is singular and does not depend on α. In this case, according to [23, 24], it may be possible to construct optimal surface $S(c_1, c_2, V) = 0$ corresponding to singular control that depends on state variables only. We use the fact that the condition $H_\alpha = 0$ implies (because of (A.4d)) that $H_0 = 0$ and also their derivatives with respect to time are equal to zero as well. We will make use of the following equations

$$H_0(c_1, c_2, V, \lambda_1, \lambda_2, \lambda_3) = 0, \tag{A.6a}$$

$$H_\alpha(c_1, c_2, V, \lambda_1, \lambda_2, \lambda_3) = 0, \tag{A.6b}$$

$$\frac{\mathrm{d}^i H_0}{\mathrm{d}t^i}(c_1, c_2, V, \alpha, \lambda_1, \lambda_2, \lambda_3) = 0, \tag{A.6c}$$

$$\frac{\mathrm{d}^i H_\alpha}{\mathrm{d}t^i}(c_1, c_2, V, \alpha, \lambda_1, \lambda_2, \lambda_3) = 0, \tag{A.6d}$$

to eliminate the adjoint variables $\lambda_1, \lambda_2, \lambda_3$ where ith order time derivatives will be considered with $i = \{1, 2, \ldots\}$ taking the necessary value. We note that it is not possible to use both conditions (A.6c) and (A.6d) simultaneously since they are linearly dependent on each other. This can be shown for $i = 1$ using (A.4d) and its time derivative

$$\frac{\mathrm{d}H}{\mathrm{d}t} = \frac{\mathrm{d}H_0}{\mathrm{d}t} + \frac{\mathrm{d}H_\alpha}{\mathrm{d}t}\alpha + H_\alpha \frac{\mathrm{d}\alpha}{\mathrm{d}t} = 0. \tag{A.7}$$

Since term $H_\alpha = 0$ it is clear that $\dot{H}_0$ and $\dot{H}_\alpha$ may not vary independently so zeroing one of these terms zeroes the other as well. This applies analogically for $i > 1$.

Optimal control in special cases. As it will be shown later, the optimal state surface will be in special cases a function of concentrations only $S(c_1, c_2) = 0$. Thus, it will be a curve in the concentration space. Once it is found, the corresponding singular control can be obtained by considering its derivative with respect to time

$$\frac{\mathrm{d}S(c_1, c_2)}{\mathrm{d}t} = \frac{\partial S}{\partial c_1}\dot{c}_1 + \frac{\partial S}{\partial c_2}\dot{c}_2 = 0. \tag{A.8}$$

Using process differential equations (1) then yields

$$\frac{\partial S}{\partial c_1}\frac{c_1 q}{V}(R_1 - \alpha) + \frac{\partial S}{\partial c_2}\frac{c_2 q}{V}(R_2 - \alpha) = 0. \tag{A.9}$$

This equation can be satisfied if α is calculated as

$$\alpha(t) = \frac{\frac{\partial S}{\partial c_1}c_1 R_1 + \frac{\partial S}{\partial c_2}c_2 R_2}{\frac{\partial S}{\partial c_1}c_1 + \frac{\partial S}{\partial c_2}c_2}. \tag{A.10}$$

Optimal control in general case. In general it might be not possible to end up with closed form representation of singular surface without using adjoint variables $\boldsymbol{\lambda}$ which trajectories are in our case not known. However, it is possible to find an expression for optimal control as a function of concentrations only.

This argument is based on a fact that optimality conditions (A.6) represent the system of equations linear in adjoint variables. By taking linear equations with zero right-hand side, it is possible to form a homogeneous system which has a non-trivial solution only if the determinant of its coefficient matrix is zero [24]. Thus by selecting three linearly independent homogeneous equations from (A.6) and by computing the determinant we find the expression for optimal control on so-called singular arc, if such exists.

The overall control strategy will not change from the previously mentioned one. In this case however, switches between constrained and singular control trajectories have to be found by other means. In our study we find them numerically by formulating a simple optimisation problem.

Appendix A.1. Minimum time problem

The Hamiltonian function for the studied problem is of the form

$$H = 1 + \lambda_1 \frac{c_1 q}{V}(R_1 - \alpha) + \lambda_2 \frac{c_2 q}{V}(R_2 - \alpha) + \lambda_3(\alpha - 1)q \tag{A.11a}$$

$$= \alpha \frac{q}{V}(-\lambda_1 c_1 - \lambda_2 c_2 + \lambda_3 V) + \frac{q}{V}(\lambda_1 c_1 R_1 + \lambda_2 c_2 R_2 - \lambda_3 V) + 1, \tag{A.11b}$$

and the adjoint variables are defined by the following differential equations

$$\dot{\lambda}_1 = -\lambda_1 \frac{1}{V}[(q + c_1 q_1)(R_1 - \alpha) + c_1 q R_{11}] - \lambda_2 \frac{1}{V}[c_2 q_1 (R_2 - \alpha) + c_2 q R_{21}] - \lambda_3(\alpha - 1)q_1, \tag{A.12a}$$

$$\dot{\lambda}_2 = -\lambda_1 \frac{1}{V}[c_1 q_2 (R_1 - \alpha) + c_1 q R_{12}] - \lambda_2 \frac{1}{V}[(q + c_2 q_2)(R_2 - \alpha) + c_2 q R_{22}] - \lambda_3(\alpha - 1)q_2, \tag{A.12b}$$

$$\dot{\lambda}_3 = \frac{q}{V^2}[\lambda_1 c_1 (R_1 - \alpha) + \lambda_2 c_2 (R_2 - \alpha)], \tag{A.12c}$$

where

$$q_1 = \frac{\partial q}{\partial c_1}, \qquad R_{11} = \frac{\partial R_1}{\partial c_1}, \qquad R_{21} = \frac{\partial R_2}{\partial c_1}, \tag{A.13a}$$

$$q_2 = \frac{\partial q}{\partial c_2}, \qquad R_{12} = \frac{\partial R_1}{\partial c_2}, \qquad R_{22} = \frac{\partial R_2}{\partial c_2}. \tag{A.13b}$$

The optimality conditions (A.6) are as follows

$$H_\alpha : \; -\lambda_1 c_1 - \lambda_2 c_2 + \lambda_3 V = 0, \tag{A.14a}$$

$$H_0 : \; \lambda_1 c_1 R_1 q + \lambda_2 c_2 R_2 q - \lambda_3 V q + V = 0, \tag{A.14b}$$

$$\frac{\mathrm{d}H_\alpha}{\mathrm{d}t} : \; \lambda_1 c_1 p_1(c_1, c_2) + \lambda_2 c_2 p_2(c_1, c_2) + \lambda_3 V p_3(c_1, c_2) = 0, \tag{A.14c}$$

where

$$p_i(c_1, c_2) = R_i(q + c_1 q_1 + c_2 q_2) + q(c_1 R_{i1} + c_2 R_{i2}) \quad i = 1, 2 \tag{A.15a}$$

$$p_3(c_1, c_2) = -(q + c_1 q_1 + c_2 q_2). \tag{A.15b}$$

For the next step, we use equations (A.14a) and (A.14c) which let us, after some manipulations, arrive at condition

$$S = \lambda_1 c_1 S_1 + \lambda_2 c_2 S_2 = 0, \tag{A.16}$$

where S_1 and S_2 are given as

$$S_1(c_1, c_2) = (R_1 - 1)(q + c_1 q_1 + c_2 q_2) + q(c_1 R_{11} + c_2 R_{12}), \tag{A.17a}$$

$$S_2(c_1, c_2) = (R_2 - 1)(q + c_1 q_1 + c_2 q_2) + q(c_1 R_{21} + c_2 R_{22}). \tag{A.17b}$$

Since (A.16) depends on unknown trajectories of adjoint variables it might be in general very difficult (maybe even impossible) to find concentration trajectory along which this equation is satisfied. However, there are some cases when it will be easily satisfied:

- $R_1 = 1$ ($R_{11} = R_{12} = 0$). This represents a common situation for a macro-solute that does not get through the membrane and micro-solute can have arbitrary properties. The optimal curve is given as

$$S(c_1, c_2) = (R_2 - 1)(q + c_1 q_1 + c_2 q_2) + q(c_1 R_{21} + c_2 R_{22}) = 0, \tag{A.18}$$

- both $R_1 \leq 1, R_2$ are constant ($R_{ij} = 0$). If both retention coefficients R_1 and R_2 are constant and do not depend on concentrations (for example a perfect membrane with $R_1 = 1$, $R_2 = 0$) the optimal curve is given as

$$S(c_1, c_2) = q + c_1 q_1 + c_2 q_2 = 0. \tag{A.19}$$

In both these special cases we can proceed to find expressions for optimal control (7) and use directly the optimal control procedure as stated above. In order to advance in the general case we will further differentiate w.r.t. time the equation (A.16) (note that this is equivalent to taking the second order time derivative of (A.6b)). This differentiation yields

$$\lambda_1 c_1(a_1\alpha + b_1) + \lambda_2 c_2(a_2\alpha + b_2) + \lambda_3 V b_3 = 0, \tag{A.20}$$

where expressions a_i and b_i for $i = 1, 2$ are given as follows

$$a_i = -c_1 q\frac{\partial S_i}{\partial c_1} - c_2 q\frac{\partial S_i}{\partial c_2}, \tag{A.21a}$$

$$b_i = c_1\left(qR_1\frac{\partial S_i}{\partial c_1} - (qR_{i1} + R_i q_1)S_1\right) + c_2\left(qR_2\frac{\partial S_i}{\partial c_2} - (qR_{i2} + R_i q_2)S_2\right), \tag{A.21b}$$

and

$$b_3 = c_1 q_1 S_1 + c_2 q_2 S_2. \tag{A.21c}$$

By writing equations (A.14a), (A.14c) and (A.20) together we recognize homogeneous system of linear equations in variables $\lambda_1 c_1$, $\lambda_2 c_2$ and $\lambda_3 V$. Such a system possesses a non-trivial solution only if determinant of its coefficient matrix is equal to zero. Using this and after some rearrangement we arrive at expression for optimal control

$$\begin{vmatrix} 1 & 1 & -1 \\ S_1 & S_2 & 0 \\ a_1\alpha + b_1 & a_2\alpha + b_2 & b_3 \end{vmatrix} = 0 \;\Rightarrow\; \alpha = \frac{(S_1 - S_2)b_3 + S_1 b_2 - S_2 b_1}{S_2 a_1 - S_1 a_2}. \tag{A.22}$$

Appendix A.2. Minimum diluant problem

The Hamiltonian function for the diluant problem is of the form

$$H = \alpha q + \lambda_1\frac{c_1 q}{V}(R_1 - \alpha) + \lambda_2\frac{c_2 q}{V}(R_2 - \alpha) + \lambda_3(\alpha - 1)q \tag{A.23a}$$

$$= \alpha\frac{q}{V}(-\lambda_1 c_1 - \lambda_2 c_2 + \lambda_3 V + V) + \frac{q}{V}(\lambda_1 c_1 R_1 + \lambda_2 c_2 R_2 - \lambda_3 V), \tag{A.23b}$$

where the adjoint variables are defined by the following differential equations

$$\dot{\lambda}_1 = -\alpha q_1 - \lambda_1 \frac{1}{V}[(q + c_1 q_1)(R_1 - \alpha) + c_1 q R_{11}] - \lambda_2 c_2 \frac{1}{V}[q_1(R_2 - \alpha) + q R_{21}] - \lambda_3(\alpha - 1)q_1, \tag{A.24a}$$

$$\dot{\lambda}_2 = -\alpha q_2 - \lambda_1 c_1 \frac{1}{V}[q_2(R_1 - \alpha) + q R_{12}] - \lambda_2 \frac{1}{V}[(q + c_2 q_2)(R_2 - \alpha) + c_2 q R_{22}] - \lambda_3(\alpha - 1)q_2, \tag{A.24b}$$

$$\dot{\lambda}_3 = \frac{q}{V^2}[\lambda_1 c_1(R_1 - \alpha) + \lambda_2 c_2(R_2 - \alpha)], \tag{A.24c}$$

and variables q_i, R_{ij} are defined in (A.13). The optimality conditions (A.6) are as follows

$$H_\alpha : \ -\lambda_1 c_1 - \lambda_2 c_2 + \lambda_3 V + V = 0, \tag{A.25a}$$

$$H_0 : \lambda_1 c_1 R_1 + \lambda_2 c_2 R_2 - \lambda_3 V = 0, \tag{A.25b}$$

$$\frac{\mathrm{d}H_0}{\mathrm{d}t} : \lambda_1 c_1 m_1(c_1, c_2) + \lambda_2 c_2 m_2(c_1, c_2) - \lambda_3 V = 0, \tag{A.25c}$$

where

$$m_1(c_1, c_2) = 1 - c_1 R_{11} - c_2 R_{12}, \tag{A.26a}$$

$$m_2(c_1, c_2) = 1 - c_1 R_{21} - c_2 R_{22}. \tag{A.26b}$$

Using equations (A.25b) and (A.25c) we can arrive at condition

$$S = \lambda_1 c_1 S_1 + \lambda_2 c_2 S_2 = 0, \tag{A.27}$$

where $S_1 = R_1 - m_1$ and $S_2 = R_2 - m_2$. Again, validity of this equation depends on adjoint variables except for special cases:

- $R_1 = 1$ ($R_{11} = R_{12} = 0$). The optimal curve is given as

$$S(c_1, c_2) = R_2 - 1 + c_1 R_{21} + c_2 R_{22} = 0, \tag{A.28}$$

- either $R_1 \neq 1$ or R_2 is constant. The optimal surface does not exist and the optimal control is of bang-bang type.

As in previous problem, if optimal surface exists, a control which will maintain optimal concentrations can be found by further differentiation (w.r.t. time) of (A.27). If it is not the case, we choose system of three linearly independent homogeneous equations (A.25a), (A.25c) and time derivative of (A.27) to form a coefficient matrix. Its determinant gives the condition for optimal control along singular arc

$$\alpha = \frac{b_2 S_1 - b_1 S_2}{a_1 S_2 - a_2 S_1}, \tag{A.29}$$

where

$$a_i = -c_1 \frac{\partial S_i}{\partial c_1} - c_2 \frac{\partial S_i}{\partial c_2}, \tag{A.30a}$$

$$b_i = c_1 R_1 \frac{\partial S_i}{\partial c_1} + c_2 R_2 \frac{\partial S_i}{\partial c_2} - c_1 R_{i1} S_1 - c_2 R_{i2} S_2. \tag{A.30b}$$